Plasma-assisted conversion of CO_2 in a dielectric barrier discharge reactor: understanding the effect of packing materials

Danhua Mei[1, 2], Xinbo Zhu[1], Yaling He[2], Joseph D. Yan[1], Xin Tu[1*]

1. Department of Electrical Engineering and Electronics, University of Liverpool, Liverpool, L69 3GJ, UK

2. Key Laboratory of Thermo-Fluid Science and Engineering of MOE, School of Energy and Power Engineering, Xi'an Jiaotong University, Xi'an, 710049, China

Corresponding author

Dr. Xin Tu

Department of Electrical Engineering and Electronics,

University of Liverpool

Liverpool L69 3GJ

UK

Submitted to the special issue of ESCAMPIG2014

Abstract

A cylindrical dielectric barrier discharge (DBD) reactor has been developed for the conversion of undiluted CO_2 into CO and O_2 at atmospheric pressure and low temperatures. Both the physical and chemical effects on reaction performance have been investigated for the addition of $BaTiO_3$ and glass beads into the discharge gap. The presence of these packing materials in the DBD reactor changes the physical characteristics of the discharge and leads to a shift of the discharge mode from a typical filamentary discharge with no packing to a combination of filamentary discharge and surface discharge with packing. Highest CO_2 conversion and energy efficiency are achieved when the $BaTiO_3$ beads are fully packed into the discharge gap. It is found that adding the $BaTiO_3$ beads into the plasma system enhances the average electric field and mean electron energy of the CO_2 discharge by a factor of 2, which significantly contributes to the enhancement of CO_2 conversion, CO yield and energy efficiency of the plasma process. In addition, highly energetic electrons (> 3.0 eV) generated by the discharge could activate $BaTiO_3$ photocatalyst to form electron-hole pairs on its surface, which contributes to the enhanced conversion of CO_2.

Keywords

CO_2 conversion; Dielectric barrier discharge; Packed-bed effect; Packing materials

1. Introduction

Carbon dioxide (CO_2) has been recognised as one of the major contributors to the greenhouse gas effect and its concentration in atmosphere is continuously increasing due to the use of fossil fuels. The UK emits more than 470 million tonnes of CO_2 per year and of this 39 % is emitted by the energy and chemistry sectors [1]. Great efforts have been devoted to the development of effective strategies to deal with the global challenge of CO_2 emission, including carbon capture and storage (CCS) [2], carbon capture and utilisation (CCU) [3], reducing fossil fuel consumption and boosting clean and renewable energy use [4]. Undoubtedly, CO_2 conversion and utilisation could be one of the attractive and sustainable solutions for the mitigation of CO_2 emissions, by turning CO_2 from a waste gas into an integral part of industrial processes. Various processes have been used to convert CO_2 into value-added fuels and chemicals, such as CO_2 reforming of CH_4 for hydrogen production, CO_2 hydrogenation for the synthesis of methanol, methane, formaldehyde, dimethyl ether, etc [5, 6]. Direct splitting of CO_2 into CO has also attracted great interest [7, 8], as CO is a useful chemical feedstock which can be used as a reactant to produce higher energy products. However, due to the high stability of CO_2, large amount of energy is required for the activation of CO_2 in the conventional CO_2 conversion process. For example, thermodynamic equilibrium calculation of CO_2 conversion shows that CO_2 begins to decompose into CO and O_2 near 2000 K with a very low conversion rate (< 1%). Reasonable conversion of CO_2 (~60%) can only be obtained at an extraordinary high temperature (3000-3500 K).

Non-thermal plasma technology has been considered as an attractive alternative to the conventional thermal or catalytic route for gas purification and energy conversion [9-14] due to its non-equilibrium character, low energy cost and unique ability to initiate both physical and chemical reactions at low temperatures [15, 16]. In a non-thermal plasma, the overall gas kinetic temperature remains low, while the electrons are highly energetic with a typical electron temperature of 1-10 eV, which can breakdown most chemical bonds of inert molecules (e.g. CO_2) and generate a large

number of reactive species for chemical reactions. The non-equilibrium character of such plasma could overcome thermodynamic barriers in chemical reactions (e.g. direct CO_2 decomposition) and enable thermodynamically unfavourable chemical reactions to occur at atmospheric pressure and low temperatures [15].

Up until now, several different types of plasma have been used for CO_2 conversion, including dielectric barrier discharges (DBDs), corona discharges, glow discharges, microwave discharges, radio frequency discharge and gliding arc discharges [17-28]. Most of previous works in this area mainly focused on the conversion of diluted CO_2 into CO and O_2. Inert gases such as He, Ar and N_2 were used as the dilution gases to assist CO_2 conversion [21]. Indarto et al investigated the effect of N_2, O_2, air and H_2O on the conversion of CO_2 in a gliding arc plasma reactor [27, 29]. Only N_2 was found to give a positive effect on CO_2 conversion. CO_2 conversion of 35% was achieved at a N_2 concentration 95% in the mixture feed gas, much higher than that in a pure CO_2 reaction (only 15-18%). However, the presence of N_2 in CO_2 reaction inevitably generates unwanted by-products such as NO_x. Similarly, Zheng et al reported that CO_2 conversion was much higher in the Ar system than that in the O_2 system in a DBD reactor [30]. To further improve the conversion of CO_2 and energy efficiency of the plasma process, different non-conductive materials have been introduced into the plasma system. Porous Al_2O_3 (α-Al_2O_3 and γ-Al_2O_3) were packed into a pulsed corona discharge reactor for CO_2 conversion and γ-Al_2O_3 was found to enhance CO_2 conversion due to its high surface area and strong adsorption capability [31]. Yu et al investigated the decomposition of CO_2 in a packed bed DBD reactor using silica gel, quartz, α-Al_2O_3, γ-Al_2O_3, $CaTiO_3$ as packing materials [32]. A series of $Ca_xSr_{(1-x)}TiO_3$ with and without additive were used as a dielectric barrier for the splitting of CO_2 in a DBD reactor [33-35]. In their works, the high permittivity of the dielectrics led to an increasing in the plasma power with very dense and strong microdischarges, which significantly enhances the conversion of CO_2. These findings suggest that the interactions between plasma and packing materials play an important role in the plasma conversion of CO_2. However, a fundamental understanding of the interaction between plasma and packing materials

from both a physical and chemical perspective is still very patchy, especially the influence of packing materials on the physical characteristics (e.g. electric field, mean electron energy) of the discharge and consequent plasma chemical reactions is still not clear and has been paid less attention.

In this study, direct conversion of undiluted CO_2 into CO and O_2 is carried out in a cylindrical DBD reactor with and without packing at low temperatures. The effect of glass and $BaTiO_3$ beads on the physical characteristics of the discharge and chemical reaction performance is investigated to get a better understanding of plasma interactions with packing materials in CO_2 conversions.

2. Experimental

2.1 Experimental setup

The experiment is carried out in a cylindrical DBD reactor, as shown in figure 1. A 6 cm long stainless steel mesh is wrapped over a quartz tube with an external diameter of 25 mm and an inner diameter of 22 mm. A stainless steel rod with an outer diameter of 16 mm is placed in the centre of the quartz tube and acted as an inner electrode. As a result, the discharge gap is 3 mm with a discharge volume V of 10.1 ml. The inner electrode is connected to a high voltage output and the outer electrode is grounded via an external capacitor C_{ext} (0.47 μF). CO_2 is used as the feed gas without dilution and the flow rate is fixed at 50 ml/min. The DBD reactor is supplied by an AC high voltage power supply with a maximum peak voltage of 30 kV and a frequency of 5-20 kHz. The applied voltage (U_a) is measured by a high voltage probe (Testec, HVP-15HF), while the current (I_t) is recorded by a current monitor (Bergoz CT-E0.5). The voltage (U_c) on the external capacitor is measured to obtain the charge generated in the discharge. All the electrical signals are sampled by a four-channel digital oscilloscope (TDS2014). The discharge power is obtained by the area calculation of the Q-U Lissajous figure. Different packing materials ($BaTiO_3$ and glass beads) of 1 mm in diameter are fully packed into the discharge volume. In this case, the reactor can be

considered as a typical packed bed DBD system. For comparison, CO_2 conversion is also carried out in the DBD reactor with no packing. The gas temperature in the DBD reactor is measured by a fiber optic temperature probe (Omega, FOB102). The gas products are analysed by a two-channel gas chromatography (Shimadzu 2014) equipped with a flame ionisation detector (FID) and a thermal conductivity detector (TCD). The concentration of ozone is measured by an ozone monitor (2B, Model 106-M).

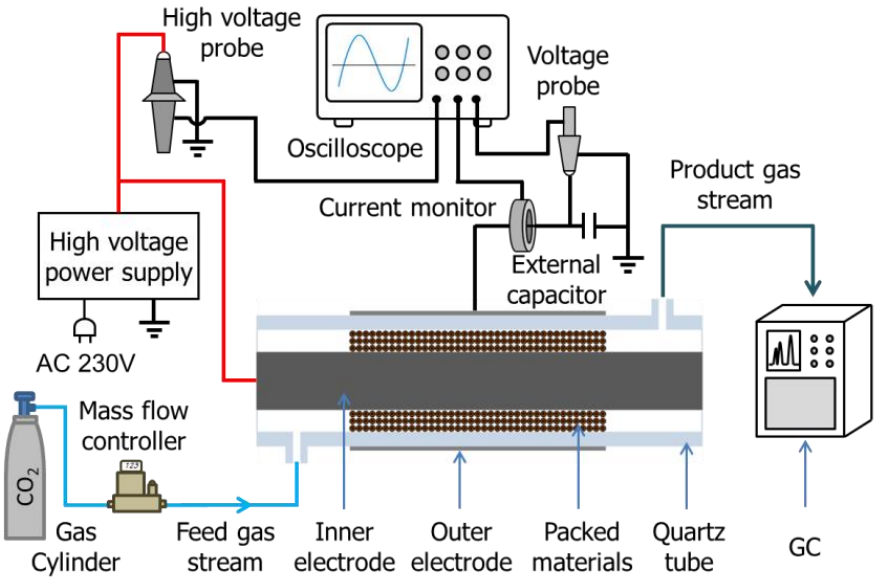

Figure 1. Schematic diagram of the experimental setup

2.2 Parameter calculation

An equivalent electrical circuit model of the DBD reactor containing two capacitors in a series connection was described in our previous paper [16]. One of the capacitors C_d represents the capacitance of the quartz tube and the other is the capacitance of the gap C_{gap}. The equivalent capacitance of the quartz tube C_d is 96.58 pF, which is calculated according to the topology of a coaxial capacitor, as shown in Equation (1) [36]:

$$C_d = \frac{2\pi\varepsilon_0\varepsilon l}{\ln\left((d+x)/d\right)} \quad (1)$$

where ε_0 is the dielectric constant of vacuum (8.854 $\times 10^{-12}$ F/m); ε is the relative dielectric constant of quartz tube (3.70); l is the discharge length; d and x are the inner diameter and wall thickness of the quartz tube, respectively, as shown in figure 2.

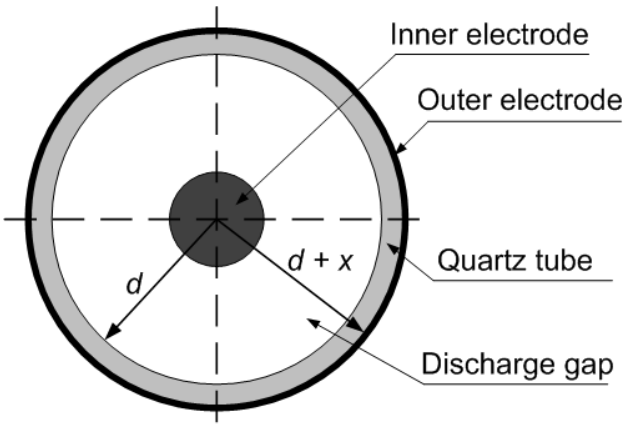

Figure 2. Transversal section of the DBD reactor with no packing

Figure 3 shows a typical *Q*-*U* Lissajous figure for a DBD reactor. Lines BC and AD represent the discharge-off phase when there is only displacement current and their slopes correspond to the C_{cell} in the plasma-off period. Lines AB and CD represent the discharge-on phase when the gas breakdown occurs in the gap and the plasma is ignited. The slope of Lines AB and CD is effective capacitance C_{eff}, which should equal C_d for a fully bridged gap [37]. The detailed examination of the *Q*-*U* plot and calculation for the capacitance of the gap C_{gap} in the discharge-off phase, the charge Q flowing through the DBD cell, the voltage on the dielectric materials U_d, the voltage across the gap U_{gap} and the breakdown voltage U_B can be found in our previous paper [16]. The peak-to-peak voltage ($Q_{pk\text{-}pk}$), charge discharged (Q_d) and charge transferred per half-cycle (Q_{trans}) can be obtained from the Lissajous figure, as plotted in figure 3 [38].

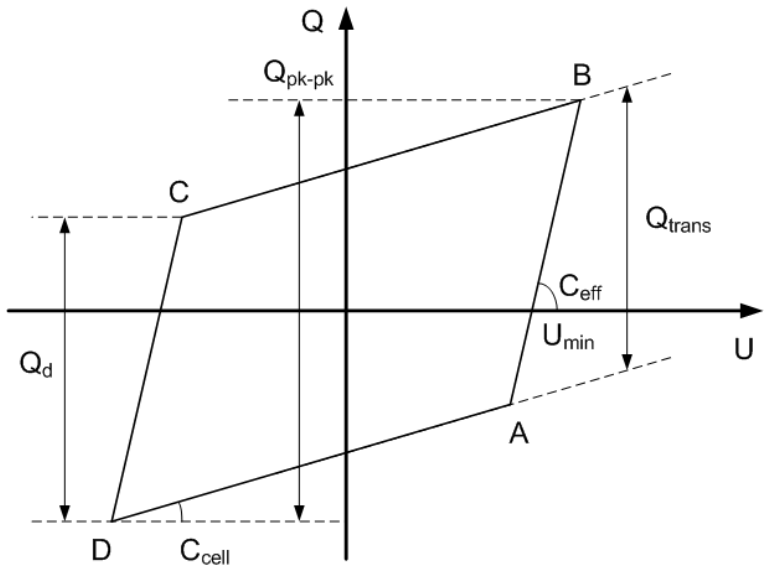

Figure 3. Typical Lissajous figure of a DBD

In the presence of packing pellets in the discharge gap, C_{gap} represents the capacitance of gas-solid integration in the gas gap; and U_{gap} is the sum of the voltage on the gas (U_g) and packing material (U_p). In this study, the beads are tightly packed into the discharge gap. The void fraction of the DBD reactor in the presence of packing materials is defined as $1\text{-}V_p/V$ (V_p is the total volume of packing beads), which is about 0.283 for the fully packing of glass or $BaTiO_3$ beads into the DBD reactor. To understand the effect of packing materials on the physical characteristics of the discharge, a simplified model has been established to determine the voltage across the gas and solid, respectively. The region of solid beads and gas is equivalently considered as two parallel plate capacitors, as shown in figure 4. The equivalent gap thicknesses in the gas (d_g) and solid (d_p) region are determined by equations (2) and (3):

$$d_g = \frac{2V_d \times \alpha}{\pi(D+d)} \tag{2}$$

$$d_p = d_{gap} - d_g \tag{3}$$

where V_d is the discharge volume; D is the outer diameter of the inner electrode.

The equivalent capacitances of the gas (C_g) and solid (C_p) regions are calculated in the form of a parallel plate capacitor:

$$C_g = \frac{\varepsilon_g \cdot \varepsilon_0 \cdot S}{d_g} \tag{4}$$

$$C_p = \frac{\varepsilon_p \cdot \varepsilon_0 \cdot S}{d_p} \tag{5}$$

where ε_g is the relative dielectric constant of CO_2 (ε_g=1.6); ε_p is the relative dielectric constant of the packing materials (3.9 for glass bead and 10000 for $BaTiO_3$); S is the surface area of the outer electrode.

The gas voltage U_g can be obtained from the following equation:

$$U_g = \frac{Q}{C_g} = \frac{U_p \cdot C_p}{C_g} = \frac{\left(U_{gap} - U_g\right) \cdot C_p}{C_g} \tag{6}$$

Equation (6) can be rewritten in the following form by introducing equations (4) and (5):

$$U_g = \frac{U_{gap}}{\frac{\varepsilon_g}{\varepsilon_p} \times \frac{d_p}{d_g} + 1} \tag{7}$$

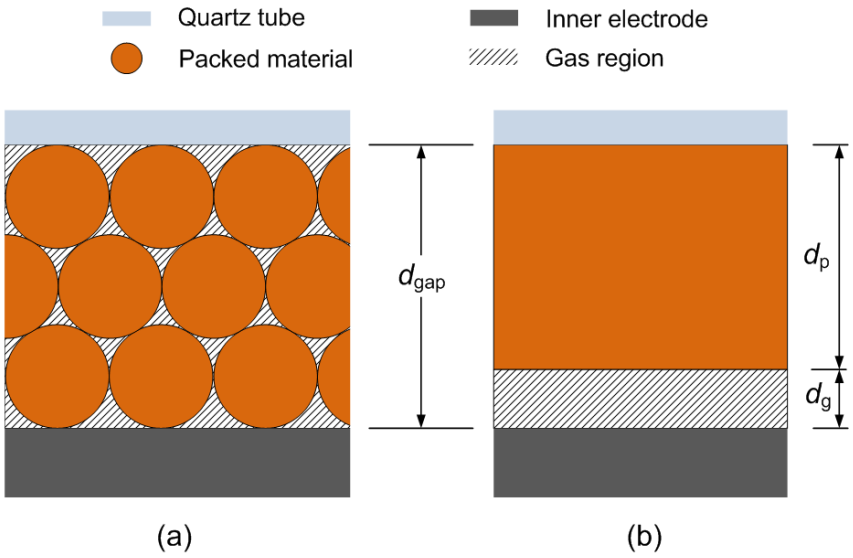

Figure 4. Simplified model for the determination of the gas gap

To evaluate the performance of the plasma process, CO_2 conversion, CO yield and selectivity are defined:

$$\mathrm{CO_2\ conversion}(\%) = \frac{\mathrm{CO_2\ converted\ (mol/s)}}{\mathrm{CO_2\ input\ (mol/s)}} \times 100 \quad (8)$$

$$\mathrm{CO\ yield}(\%) = \frac{\mathrm{CO\ formed\ (mol/s)}}{\mathrm{CO_2\ input\ (mol/s)}} \times 100 \quad (9)$$

$$\mathrm{CO\ selectivity}(\%) = \frac{\mathrm{CO\ formed\ (mol/s)}}{\mathrm{CO_2\ converted\ (mol/s)}} \times 100 \quad (10)$$

Specific energy density (SED) is defined as the ratio of the discharge power to the gas flow per unit volume:

$$\mathrm{SED(kJ/L)} = \frac{\mathrm{Discharge\ power\ (W)}}{\mathrm{CO_2\ flow\ rate\ (L/s)}} \quad (11)$$

The energy efficiency of the plasma CO_2 conversion process is defined as the number of moles of CO_2 converted per unit of plasma power:

$$\mathrm{E(mmol/kJ)} = \frac{\mathrm{CO_2\ converted\ (mol/s)}}{\mathrm{Discharge\ power\ (W)}} \quad (12)$$

3. Results and discussion

3.1 Effect of packed materials on discharge characteristics

Figure 5 presents the electrical signals of the CO_2 discharge with and without packing materials. In the discharge with no packing, a typical filamentary discharge can be clearly observed, which can also be confirmed by the numerous peaks in the current signal. In contrast, packing $BaTiO_3$ or glass beads into the entire discharge area generates a typical packed-bed effect and leads to a transition in the discharge behaviour from a filamentary discharge to a combination of surface discharge and filamentary discharge. The addition of $BaTiO_3$ or glass beads into the DBD reactor is found to significantly reduce the amplitude of the current peaks. In a packed-bed DBD reactor, filaments can only be generated in the small gap between the pellet-pellet and the pellet-quartz wall, while surface discharge can be formed on the surface of pellets near contact points between pellets. Similar findings were reported in our previous works where fully packing Ni/Al_2O_3 or TiO_2 catalyst pellets into a DBD reactor significantly changes the discharge mode and inhibits the formation of

filamentary discharges due the decrease of the discharge volume [16, 39]. However, intense filamentary discharges were still formed when quartz wool was placed in the discharge area due to the porosity of this material and strong interactions between the plasma and quartz wool [15].

Note that the gap voltage of the CO_2 discharge in the packed bed DBD reactor is much lower than that of the discharge with no packing. The breakdown voltage (U_B) of the discharge significantly decreases from 3.43 kV without packing to 1.56 kV (packed with glass beads) and 1.03 kV (packed with $BaTiO_3$), respectively. This phenomenon can be ascribed to the reduced electrode gap and reduced pressure due to the packing of solid materials into the discharge gap. Such changes were also observed in previous studies where packing a series of materials (Ni/Al_2O_3, Al_2O_3, TiO_2, and zeolite 3A) into the discharge gap showed that the influence of dielectric constant of the packing materials on the reduction of breakdown voltage was weak [16, 40, 41].

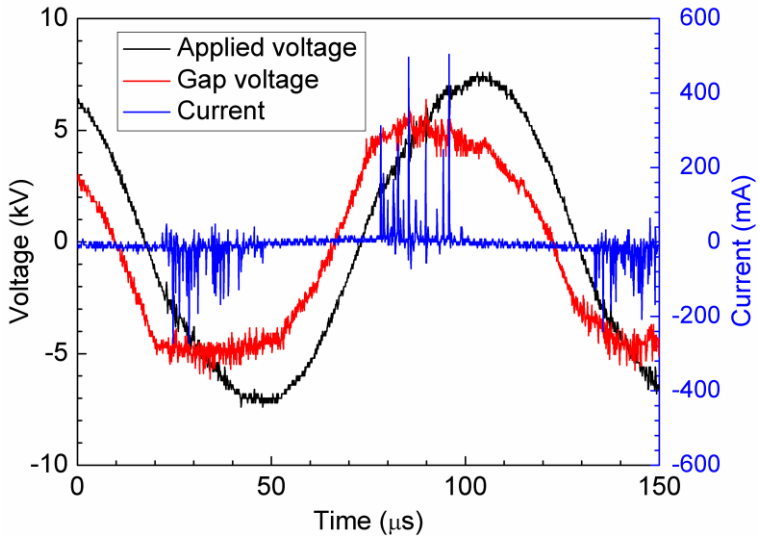

(a)

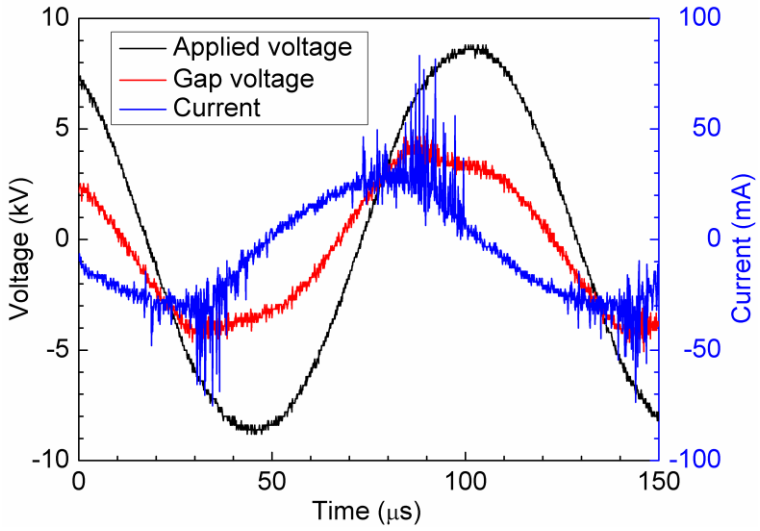

(b)

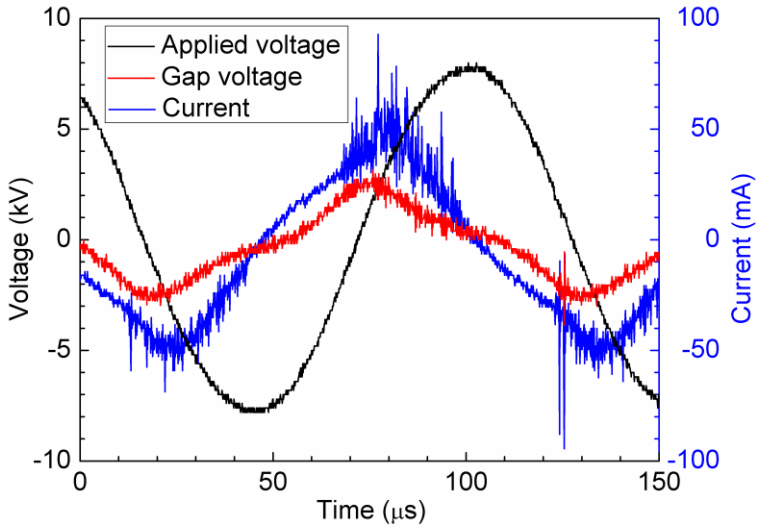

(c)

Figure 5. Electrical signals of the CO_2 DBD: (a) with no packing; (b) packed with glass beads; (c) packed with $BaTiO_3$ beads (discharge power: 40W; feed flow rate: 50 ml/min; frequency: 9 kHz; SED: 48 kJ/L)

Figure 6 shows the Lissajous figures of the CO_2 discharge with and without packing material at the same discharge power of 40 W. The shape of the Lissajous figure changes from parallelogram to oval shape when either $BaTiO_3$ or glass beads are fully packed in the DBD reactor. This also indicates the change in the discharge characteristics. At the same discharge power, the applied voltage of the DBD increases from 14.1 kV_{pk-pk} without packing to 15.3 kV_{pk-pk} with the $BaTiO_3$

packing and 16.9 kV_{pk-pk} with the glass beads packing, while the current in the discharge with no packing is much higher than that in the presence of packing beads, as shown in figure 5.

In the discharge-off phase, the total equivalent capacitance of the DBD reactor with no packing is about 13.6 pF. Adding the glass or $BaTiO_3$ beads to the plasma system significantly increases the value of this parameter to 43.8 pF and 54.4 pF, respectively. Similarly, the gap capacitance is also increased from 14.5 pF without packing to 80.2 pF and 124.6 pF when the discharge gap is fully packed with the glass or $BaTiO_3$ beads.

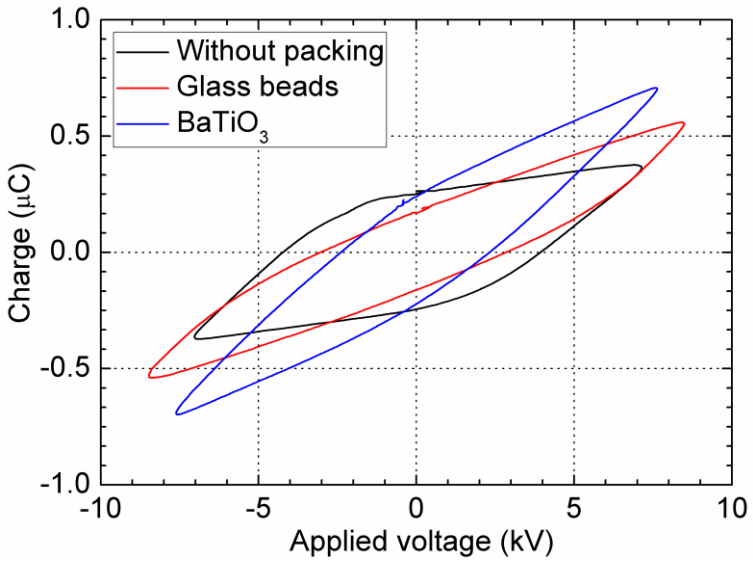

Figure 6. Lissajous figures of the CO_2 DBD without and with different packing material at a constant discharge power of 40 W (feed flow rate: 50 ml/min; frequency: 9 kHz; SED: 48 kJ/L)

The influence of the packing solids on the effective capacitance of the DBD at different discharge powers is plotted in Figure 7. Increasing the discharge power or SED enhances the effective capacitance irrespective of the use of packing materials. For example, the effective capacitance of the discharge without packing increases from 25.5 pF to 58.6 pF when the discharge power varies from 20 W to 50 W. This can be clearly seen from the slope of the lines AB and CD in the Lissajous figure. In the discharge with no packing, the effective capacitance is much lower than the

capacitance of the quartz tube (96.58 pF). This phenomenon might be caused by the incomplete formation of microdischarge in the whole discharge gap under the experimental conditions. Similar observation was reported in a CH_4/CO_2 DBD [16]. In addition, it is also suggested that C_{eff} depends on the spatial distribution of the discharge across the discharge gap over a half-period of the applied voltage. When the packing materials are placed in the reactor, the C_{eff} increases compared with that of the discharge with no packing. Interestingly, the maximum C_{eff} of 91.5 pF can be obtained when the $BaTiO_3$ beads are fully packed into the discharge gap at a discharge power of 40 W. This value is very close to the capacitance of the quartz tube. It is expected the effective capacitance should be equal to C_d for a fully bridged gap [37]. This can demonstrate that the presence of $BaTiO_3$ beads in the discharge leads to the expansion of the discharge across the gap, and might consequently affect the plasma chemical reactions.

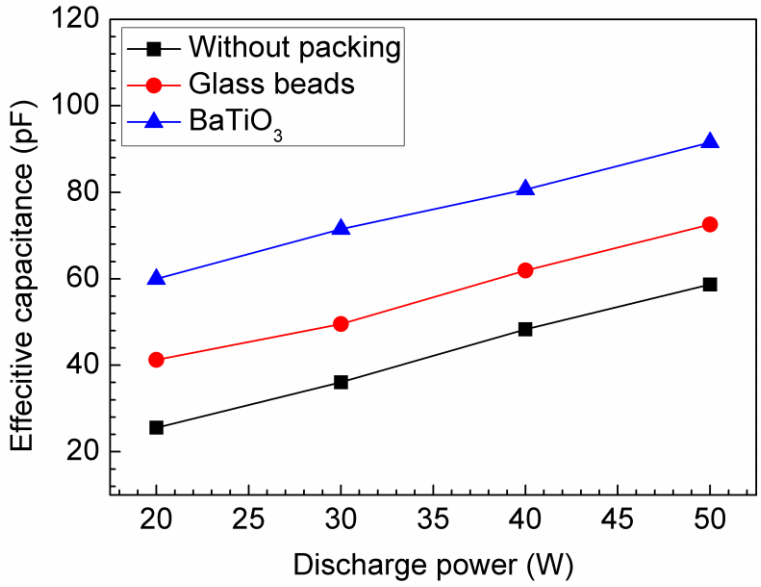

Figure 7. Effect of packing materials on the effective capacitance of the CO_2 discharge (feed flow rate: 50 ml/min; frequency: 9 kHz; SED: 24 – 60 kJ/L)

Figure 8 shows the influence of the packing materials on the charge characteristics of the CO_2 DBD at different discharge powers. It is found that the peak-to-peak charge increases with the increase in the discharge power. Both charge generated and transferred per half-cycle of the applied voltage

also increase with the discharge power. Similar evolution was observed in previous studies where these charge parameters increased with the discharge power in a plasma methane reforming process [16]. The addition of the packing materials to the DBD reactor has a significant effect on the charge characteristics of the CO_2 discharge. Both packing materials are found to bridge the gap between the electrodes and enhance the charge transfer between them.

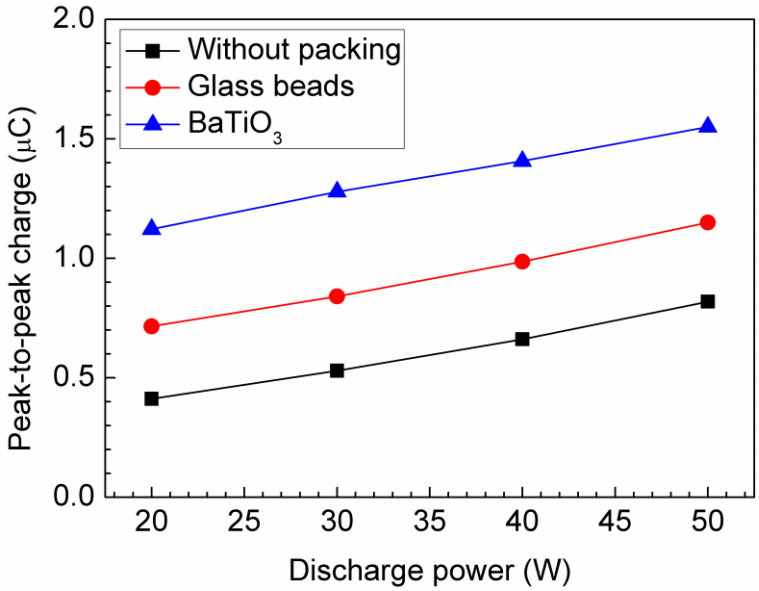

(a)

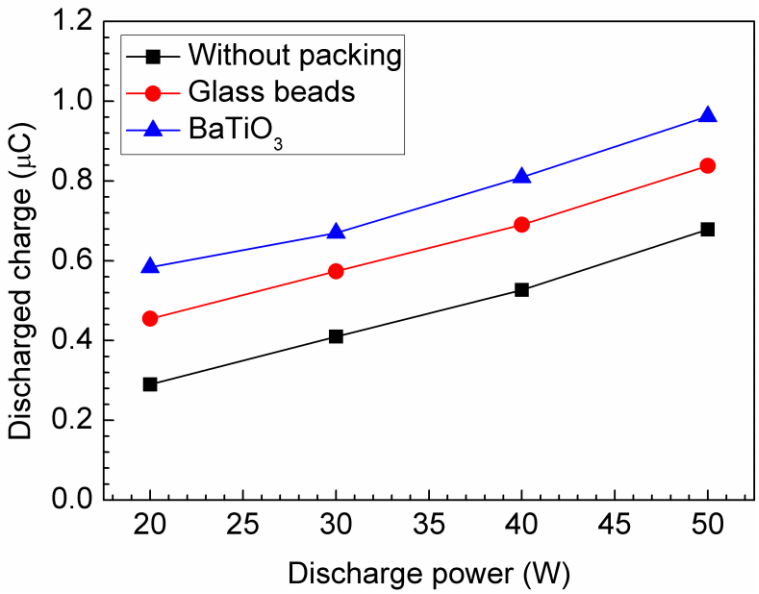

(b)

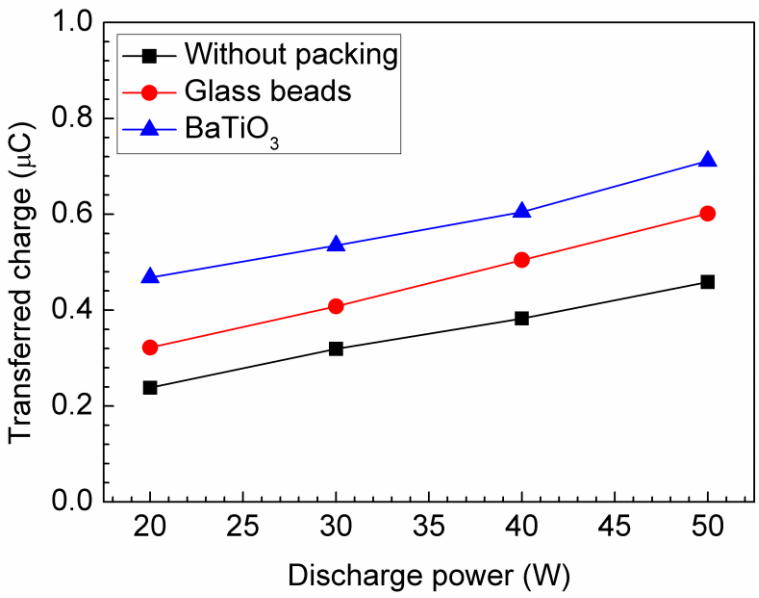

(c)

Figure 8. Effect of packing materials on the charge generation and transfer in the pure CO_2 DBD: (a) peak-to-peak charge; (b) charge generated per half-cycle; (c) charge transferred per half-cycle (feed flow rate: 50 ml/min; frequency: 9 kHz; SED: 24 – 60 kJ/L)

3.2 Effect of packing materials on electric field and electron energy

The effect of the packing materials on the average electric field strength of the discharge at different discharge powers is shown in figure 9. Clearly, increasing the discharge power effectively enhances the electric field of the CO_2 discharge regardless of the packing material used. The presence of the packing materials in the discharge also significantly improves the average electric field strength. The material ($BaTiO_3$) with a higher dielectric constant has a more significant effect on the electric field of the discharge. For example, the average electric field strength (25.01 kV/cm) in the DBD reactor fully packed with the $BaTiO_3$ beads is almost doubled compared to that of the discharge with no packing (12.90 kV/cm) at the same discharge power of 50 W. A similar finding was reported in [42] where the presence of TiO_2 pellets in a nitrogen DBD led to a significant increase of the electric field. Previous experimental [43, 44] and simulation studies [45, 46] showed that packing solid pellets especially the pellets with a high dielectric constant (e.g., $BaTiO_3$) into the discharge gap significantly enhanced the local electric field strength near contact points between the

pellets and the pellet – dielectric wall. The maximum local electric field near these contact points can be 10 – 10^4 times higher than that in the void in a plasma-catalysis system, depending on the properties of the packing materials such as contact angle, shape and dielectric constant, while the averaged electric field in an argon plasma fully packed with packing pellets was increased by a factor of 1.4 with increasing the dielectric constant of the packing materials from 10 to 1000, above this the change in the electric field became negligible [47]. Our results also show that the electric field of the CO_2 discharge is not a function of dielectric constant when the packing materials with different constants (3.9 and 10000) are fully packed in the DBD reactor. Table 1 presents the effect of the packing materials on the reduced electric field strength at different discharge powers. Similarly, increasing the plasma power significantly enhances the reduced electric field of the discharge, while the presence of the glass or $BaTiO_3$ beads in the plasma system leads to a higher reduced electric field.

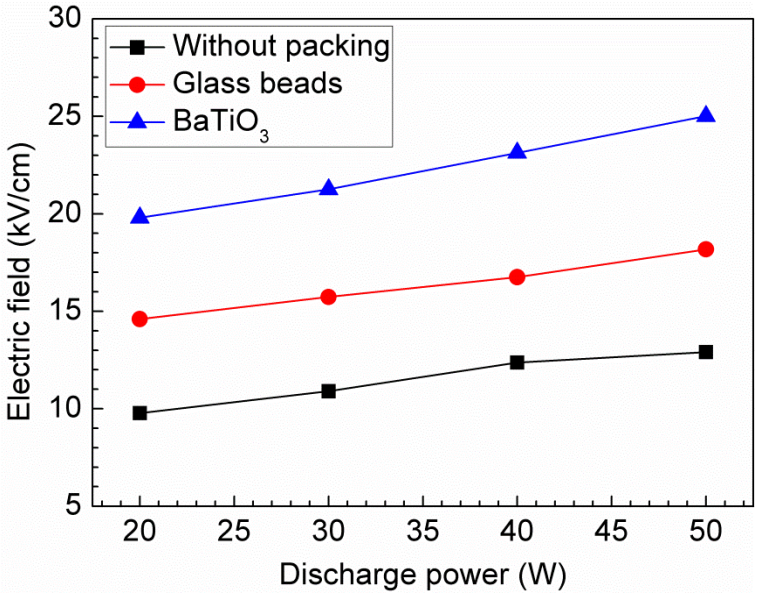

Figure 9. Effect of packing materials on the average electric field strength at different discharge powers (feed flow rate: 50 ml/min; frequency: 9 kHz; SED: 24 – 60 kJ/L)

Table 1. Effect of packing materials on *E*/*N* at different discharge powers

Discharge power (W)	*E*/*N* (Td)		
	Without packing	Glass beads	$BaTiO_3$ beads
20	36.38	54.32	73.64
30	40.54	58.50	79.07
40	46.02	62.30	86.04
50	47.99	67.62	93.02

The electron energy distribution function (EEDF) of the CO_2 discharge under our experimental conditions is calculated by BOLSIG+ [48]. Figure 10 shows the mean electron energy as a function of the reduced electric field (E/N). The effect of the packing solids on the mean electron energy of the discharge has also been investigated, as shown in figure 11. Clearly, increasing the plasma power or SED leads to generate more electrons with higher energy. Packing the $BaTiO_3$ pellets in the discharge gap almost doubles the mean electron energy at the discharge power of 50 W, while the mean electron energy of the discharge with glass beads is increased by around 46.23%. In our previous study, we reported that the integration of plasma and TiO_2 strongly affected the electron energy distribution in a N_2 discharge with an increase in both highly energetic electrons and electric field strength [39]. These results suggest that the presence of solid pellets in the discharge gap play a crucial role in inducing physical effects, such as the enhancement of electric field and mean electron energy, which in turn produces more energetic electrons and chemically reactive species for plasma reactions and consequently contributes to the conversion of CO_2.

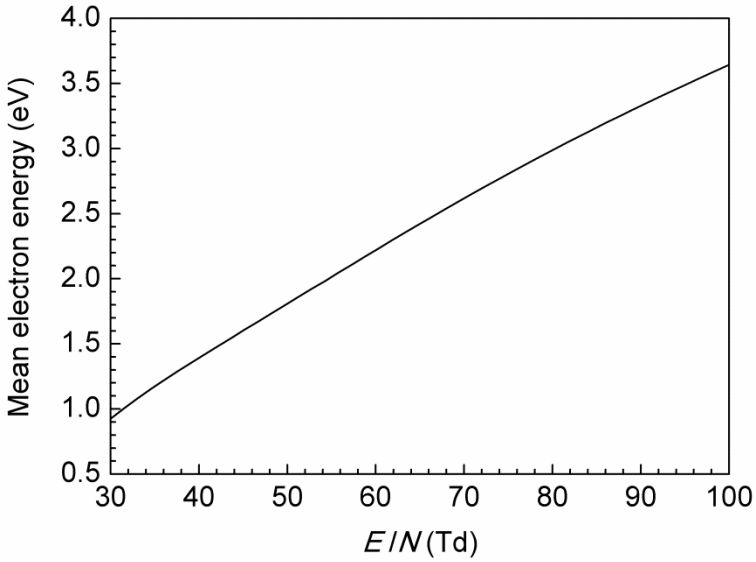

Figure 10. Mean electron energy in the CO_2 DBD as a function of E/N

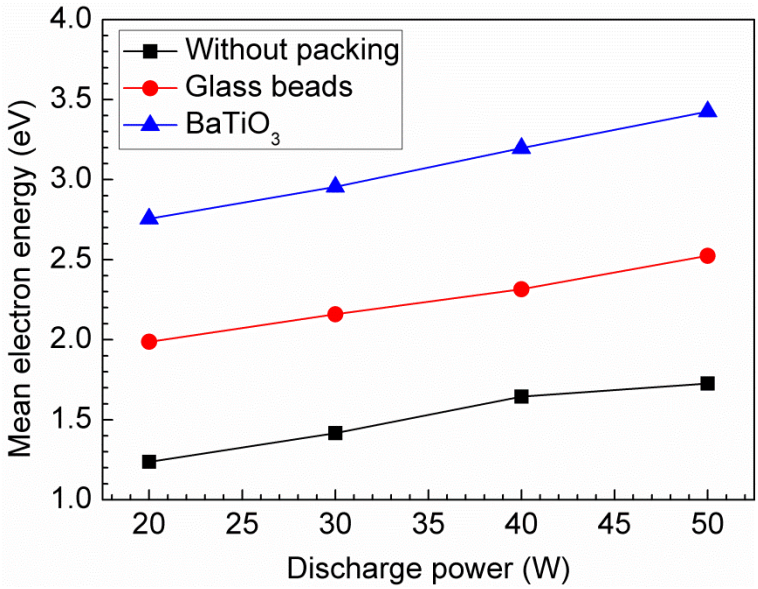

Figure 11. Effect of packing materials on the mean electron energy in the CO_2 DBD at different discharge powers (feed flow rate: 50 ml/min; frequency: 9 kHz; SED: 24 – 60 kJ/L)

3.3 Effect of packing materials on CO_2 conversion

Plasma conversion of CO_2 is carried out in the DBD reactor with and without packing material. CO_2 conversion increases with the increase of the discharge power, as shown in figure 12. Our calculation has shown that increasing the plasma power or SED effectively enhance the average electric field and mean electron energy in the discharge, all of which can generate more energetic

electrons and reactive species for plasma chemical reaction, consequently improves the conversion of CO_2. The presence of the packing materials in the discharge gap makes the reactor more effective for CO_2 conversion, even though fully packing these packing beads into the discharge gap significantly decreases the residence time of CO_2 molecules in the discharge area from 12.89 s with no packing to 3.65 s with packing. It is worth noting that plasma-induced adsorption and desorption of CO_2 on the $BaTiO_3$ surface may prolong the retention time of CO_2 in the discharge and partly compensate the reduced of CO_2 residence time due to the decrease of the discharge volume. Compared to the plasma reaction with no packing, the addition of $BaTiO_3$ and glass beads to the plasma system increases the conversion of CO_2 by around 75 % and 35%, respectively. It is found that the conversion of CO_2 is not a function of dielectric constant when the packing pellets with different dielectric constants are placed in the plasma reactor. The enhancement of CO_2 conversion is mainly attributed to the changes in the discharge characteristics, such as the increase of the average electric field and mean electron energy when solid pellets are packed into the discharge volume, as shown in figures 9 and 11. However, with the $BaTiO_3$ packing, the contribution of plasma photocatalytic surface reaction to the enhancement of CO_2 conversion cannot be ruled out [49]. It is believed that plasma discharges can generate strong UV radiation without using extra UV sources (e.g. UV lamps) to activate photocatalysts such as $BaTiO_3$. Nevertheless, the contribution of this mechanism to the photocatalytic reactions is still not clear. Previous works reported that UV radiation generated by plasma discharges is not always the controlling factor to activate photocatalysts [50, 51]. In contrast, the electrons with a high energy (> 3.0 eV for $BaTiO_3$) generated by the CO_2 discharge can trigger electron impact activation of $BaTiO_3$ photocatalysts to form electron-hole pairs, which contributes to the enhanced conversion of CO_2.

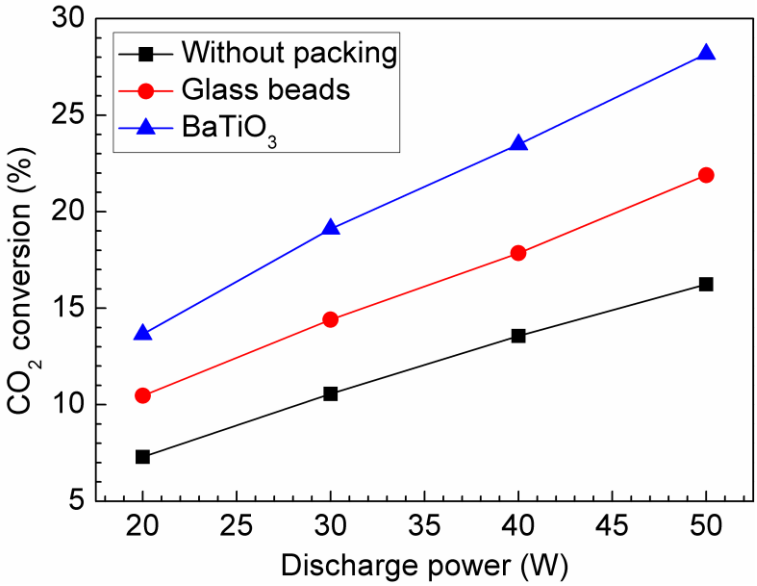

Figure 12. Effect of packing materials on CO_2 conversion (feed flow rate: 50 ml/min; frequency: 9 kHz; SED: 24 – 60 kJ/L)

Figure 13 shows the effect of the packing materials on the energy efficiency of the plasma processing of CO_2 as a function of the discharge power. Compared to the plasma reaction with no packing, the presence of $BaTiO_3$ and glass beads in the gas gap significantly enhances the energy efficiency of the plasma process. Packing the $BaTiO_3$ into the discharge leads to an increase in the energy efficiency of the process by 75% compared to the reaction with no packing at the same discharge power of 50 W. The maximum energy efficiency of 0.254 mmol/kJ is achieved when the $BaTiO_3$ pellets are fully packed into the discharge volume at a discharge power of 20 W and a feed flow rate of 50 ml/min. Figure 14 shows a comparison of the energy efficiency for CO_2 conversion using DBDs with and without packing. It is clear that there is a balance between the maximum CO_2 conversion and maximum energy efficiency of the process. Further optimisation of the plasma reactor geometry, feed conditions, different packing methods, and packing materials especially the use of suitable catalysts would be expected to improve the energy efficiency of the process with a high CO_2 conversion.

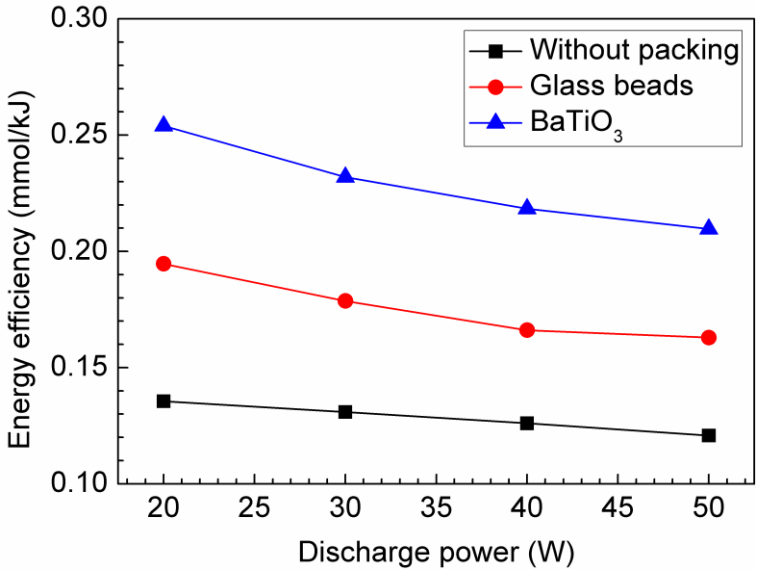

Figure 13. Effect of discharge power on energy efficiency (feed flow rate: 50 ml/min; frequency: 9 kHz; SED: 24 – 60 kJ/L)

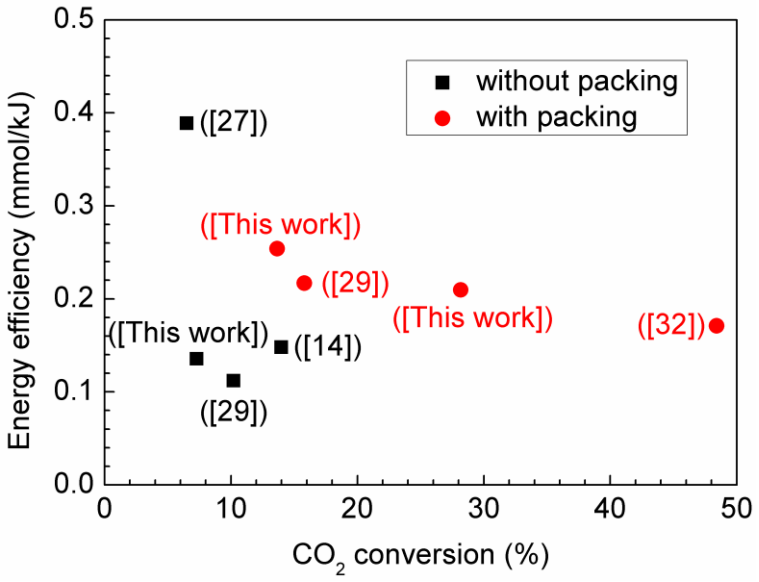

Figure 14. Comparison of energy efficiency for CO_2 conversion with different DBD reactors

The influence of the packing solids on CO selectivity and CO yield at different discharge powers is plotted in figure 15. CO selectivity is almost independent of the discharge power and packing materials, while CO yield increases with the increase of the discharge power. The presence of the $BaTiO_3$ in the discharge gap significantly enhances the yield of CO by 72.94%. The selectivity of CO based on carbon atom (equation 10) is close to 100%, which suggests that stoichiometric

conversion of CO_2 to CO is achieved in this study. This can be confirmed by the linear relationship between the CO_2 conversion and CO yield (see figure 16), which suggests that the production of CO mainly comes from the dissociation of CO_2. The electron impact dissociation of CO_2 will most likely result in CO in its ground state ($^1\Sigma$) and O atoms in both the ground state (^3P) and the metastable state (^1D). However, previous work reported that CO can also be formed in excited state since CO bands were observed [15]. The stoichiometric conversion of CO_2 to CO can be further demonstrated by the fact that no carbon deposition and ozone are detected in the plasma reactions. In contrast, Horvath et al found that CO and ozone were the main gas products in the decomposition of pure CO_2 by a corona discharge [20]. Mikoviny et al reported that adding trace oxygen into pure CO_2 significantly increased the concentration of ozone and CO in the CO_2 splitting using a negative corona discharge reactor [19].

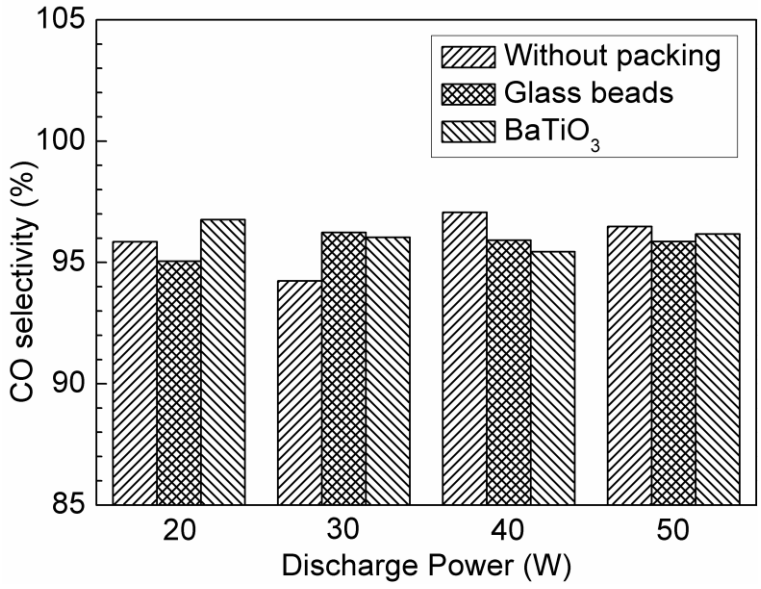

(a)

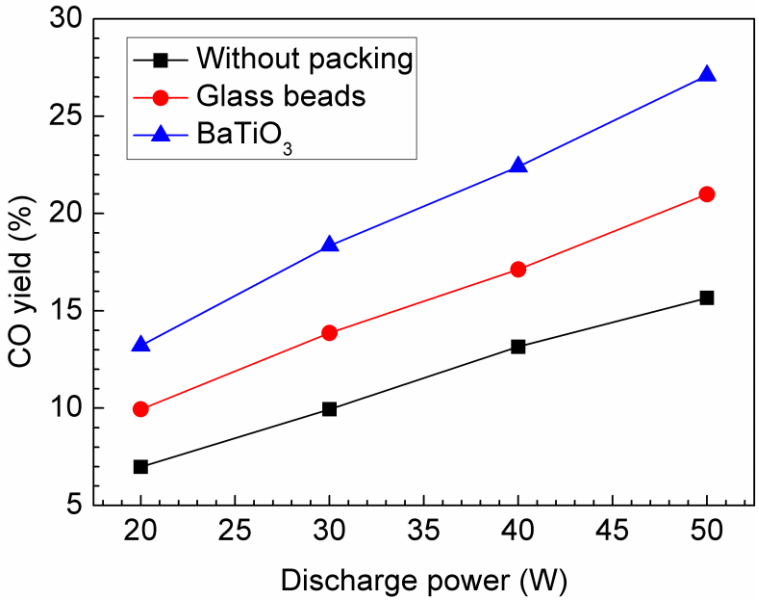

(b)

Figure 15. Effect of packing materials on (a) CO selectivity and (b) CO yield (feed flow rate: 50 ml/min; frequency: 9 kHz; SED: 24 – 60 kJ/L)

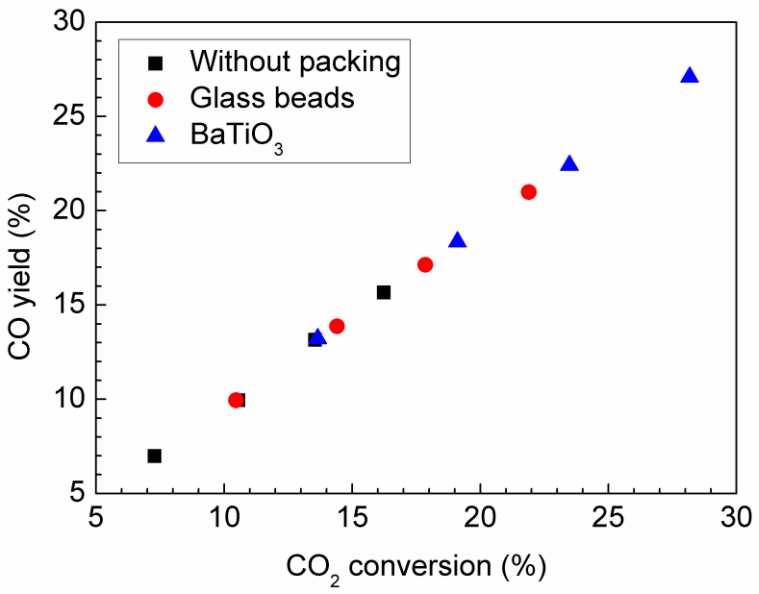

Figure 16. CO yield vs. CO_2 conversion (feed flow rate: 50 ml/min; frequency: 9 kHz; SED: 24 – 60 kJ/L)

4. Conclusions

Plasma-assisted conversion of undiluted CO_2 into CO and O_2 has been carried out in a cylindrical DBD reactor with and without packing materials. The influence of the packing materials ($BaTiO_3$

and glass beads) on the CO_2 discharge characteristics and CO_2 conversion has been investigated. The presence of $BaTiO_3$ and glass beads in the DBD reactor changes the discharge behaviour and shows a transition from a typical filamentary discharge with no packing to a combination of filamentary discharge and surface discharge at the same discharge power. The addition of BaTiO3 into the plasma system significantly enhances the average electric field and mean electron energy by 93.87% and 98.49%, respectively, which also affects the plasma chemical reactions. The use of packing materials ($BaTiO_3$ and glass beads) in the discharge gap is found to make the DBD reactor more effective for CO_2 conversion even though the residence time of CO_2 in the discharge is reduced due to the .decrease of the discharge volume at the same gas flow rate. Compared to the plasma CO_2 conversion with no packing, the presence of $BaTiO_3$ beads in the DBD reactor significantly increases the conversion of CO_2 by 75 %. These results indicate that the change of the discharge properties (e.g. electric field and mean electron energy) significantly enhances CO_2 conversion, CO yield and energy efficiency of the plasma process. In addition, highly energetic electrons (> 3.0 eV) generated by the discharge could activate photocatalyst ($BaTiO_3$) to form electron-hole pairs on the surface of $BaTiO_3$, which also contributes to the enhanced conversion of CO_2.

Acknowledgement

Support of this work by the UK EPSRC CO2Chem Network and Foundation of Key Laboratory of Thermo-Fluid Science and Engineering (Xi'an Jiaotong University), Ministry of Education (China) is gratefully acknowledged. D. H. Mei acknowledges the PhD fellowship co-funded by the Doctoral Training Programme (DTP) of the University of Liverpool and the Chinese Scholarship Council (CSC).

Reference

[1] Styring P, Jansen D, de Coninck H and Armstrong K 2011 Carbon capture and utilisation in the green economy: Using CO2 to manufacture fueld, chemicals and materils *Report* The Centre for Low Carbon Future, York
[2] Rubin E S and Zhai H B *Environ. Sci. Technol.* 2012 **46** 3076-84
[3] Abd Rahaman M S, Cheng L H, Xu X H, et al. *Renew. Sust. Energ. Rev.* 2011 **15** 4002-12
[4] Verbruggen A, Fischedick M, Moomaw W, et al. *Energ. Policy* 2010 **38** 850-61
[5] Centi G, Quadrelli E A and Perathoner S *Energy & Environ. Sci.* 2013 **6** 1711-31
[6] Lebouvier A, Iwarere S A, d'Argenlieu P, et al. *Energ. Fuel* 2013 **27** 2712-22
[7] Nordhei C, Mathisen K, Bezverkhyy I, et al. *J. Phys. Chem. C* 2008 **112** 6531-37
[8] Kim S S, Lee S M and Hong S C *J Ind. Eng. Chem.* 2012 **18** 860-64
[9] Harling A M, Glover D J, Whitehead J C, et al. *Environ. Sci. Technol.* 2008 **42** 4546-50
[10] Snoeckx R, Aerts R, Tu X, et al. *J.Phys. Chem. C* 2013 **117** 4957-70
[11] Yu L, Tu X, Li X D, et al. *J. Hazard. Mater.* 2010 **180** 449-55
[12] Aerts R, Tu X, De Bie C, et al. *Plasma Processes Polym.* 2012 **9** 994-00
[13] Tu X and Whitehead J C *Int. J. Hydrogen Energ.* 2014 **39** 9658-69
[14] Liu S Y, Mei D H, Shen Z, et al. *J. Phys. Chem. C* 2014 **118** 10686-93
[15] Tu X and Whitehead J C *Appl.Catal. B Environ.* 2012 **125** 439-48
[16] Tu X, Gallon H J, Twigg M V, et al. *J. Phys.D Appl. Phys.* 2011 **44** 274007
[17] Paulussen S, Verheyde B, Tu X, et al. *Plasma Sources Sci.Technol.* 2010 **19** 034015
[18] Aerts R, Martens T and Bogaerts A *J. Phys. Chem. C* 2012 **116** 23257-73
[19] Mikoviny T, Kocan M, Matejcik S, et al. *J. Phys. D Appl. Phys.* 2004 **37** 64-73
[20] Horvath G, Skalny J D and Mason N J *J. Phys. D Appl. Phys.* 2008 **41** 8
[21] Brock S L, Marquez M, Matejcik S, et al. *J. Catal.* 1998 **180** 225-33
[22] Wang J Y, Xia G G, Huang A M, et al. *J. Catal.*1999 **185** 152-59
[23] Tsujii M, Tanoue T, Nakano K and Nishimura Y 2001 *Chem. Lett.* **30** 22-23
[24] Sakurai T and Yokoyama A *J. Nucl. Sci. Technol.* 2000 **37** 814-20
[25] Spencer L F and Gallimore A D *Plasma Chem. Plasma Process.* 2011 **31** 79-89
[26] Hsieh L T, Lee W J, Li C T, et al. *J. Chem. Technol. Biotechnol.* 1998 **73** 432-42
[27] Indarto A, Yang D R, Choi J W, et al. *J. Hazard. Mater.* 2007 **146** 309-15
[28] Nunnally T, Gutsol K, Rabinovich A, et al. *J. Phys. D-Appl. Physi.* 2011 **44** 274009
[29] Indarto A, Choi J-W, Lee H, et al. *Environ. Eng. Sci.* 2006 **23** 1033-43
[30] Zheng G Y, Jiang J M, Wu Y P, et al. *Plasma Chem. Plasma Process.* 2003 **23** 59-68
[31] Wen Y Z and Jiang X Z *Plasma Chem. Plasma Process.* 2001 **21** 665-78
[32] Yu Q Q, Kong M, Liu T, et al. *Plasma Chem. Plasma Process.* 2012 **32** 153-63
[33] Li R X, Tang Q, Yin S, et al. *Appl. Phys. Lett.* 2007 **90** 131502
[34] Li R X, Tang Q, Yin S, et al. *Chem. Lett.* 2004 **33** 412-13
[35] Wang S, Zhang Y, Liu X L, et al. *Plasma Chem. Plasma Process.* 2012 **32** 979-89
[36] Valdivia-Barrientos R, Pacheco-Sotelo J, Pacheco-Pacheco M, et al. *Plasma Sources Sci. Technol.* 2006 **15** 237-45
[37] Francke K P, Rudolph R and Miessner H *Plasma Chem. Plasma Process.* 2003 **23** 47-57
[38] Falkenstein Z and Coogan J J *J. Phys. D Appl. Phys.* 1997 **30** 817-25
[39] Tu X, Gallon H J and Whitehead J C *J. Phys. D Appl. Phys.* 2011 **44** 482003
[40] Tu X, Verheyde B, Corthals S, et al. *Phys. Plasmas* 2011 **18** 080702
[41] Gallon H J, Tu X and Whitehead J C *Plasma Processes Polym.* 2012 **9** 90-97
[42] Guaitella O, Gatilova L and Rousseau A *Appl. Phys. Lett.* 2005 **86** 151502
[43] Gallon H J, Kim H H, Tu X, et al. *IEEE Trans. Plasma Sci.* 2011 **39** 2176-77
[44] Tu X, Gallon H J and Whitehead J C *IEEE Trans. Plasma Sci.* 2011 **39** 2172-73
[45] Kang W S, Park J M, Kim Y, et al. *IEEE Trans. Plasma Sci.* 2003 **31** 504-10
[46] Lee H M, Chen S H and Chen H L 2007 *18th International Symposium on Plasma Chemistry*

[47] Chen H L, Lee H M, Chen S H, et al. *Ind. Eng. Chem. Res.* 2008 **47** 2122-30
[48] Hagelaar G J M and Pitchford L C *Plasma Sources Sci. Technol.* 2005 **14** 722-33
[49] Devi L G and Krishnamurthy G *J. Phys. Chem. A* 2011 **115** 460-69
[50] Kim H H, Ogata A and Futamura S *J. Phys. D Appl. Phys.* 2005 **38** 1292-00
[51] Guaitella O, Thevenet F, Puzenat E, et al. *Appl.Catal. B Environ.*2008 **80** 296-05